

Assessment of Overall Thermal Performance of Conjugate Pure Mixed Convection in a Lid-Driven Partitioned Cavity

Sumon Saha, Mir Atiqur, Md Alif Mahmud and R. K. B. M. Rizmi

Department of Mechanical Engineering

Bangladesh University of Engineering and Technology (BUET)

Dhaka 1000, Bangladesh

sumonsaha@me.buet.ac.bd, miratiqrahman@gmail.com, mdalifmahmud39@gmail.com,
rkbm015@gmail.com

Abstract

Conjugate mixed convection heat transfer inside a partitioned cavity has been carried out in this work. The cavity is differentially heated, and a solid partition of finite thickness is placed vertically at the mid-section of the domain resulting two separate chambers. The cold right wall is moving on its place at a constant velocity, while the remaining walls are stationary. Two-dimensional, steady state, incompressible air flow within the system is governed by Navier-Stokes and energy equations, which are solved by finite element method. The governing parameters Reynolds and Grashof numbers are varied in such a way that the resulting mixed convection parameter (Richardson number) remains constant at unity ensuring pure mixed convection heat transfer. In order to analyze the conjugate effect of the thermal system, overall thermal performance is assessed for different governing parameters and geometric conditions of the partition. Besides, variations of streamline plots and isotherms are qualitatively visualized and compared. The distribution of average Nusselt number with both Reynolds and Grashof numbers under different conditions is also presented to evaluate the performance of convection heat transfer of the system.

Keywords

Conjugate convection, Differential heating, Overall thermal performance, Finite element method, Nusselt number

1. Introduction

Mixed convection flows occur in many technological and industrial applications in, e.g. solar receivers exposed to wind currents, electronic devices cooled by fans, nuclear reactors cooled during emergency shutdown, thick-walled ducts [1], furnace design, nuclear reactor or cooling of electronic devices [2–3]. There are many studies of mixed convection in an enclosure. But we are showing here the thermal performance of a conjugate mixed convection in a partitioned cavity. To assess the thermal performance, we changed different governing parameters and geometric conditions of the partition.

1.1 Objectives

CFD analysis for partitioned cavity was carried out in this study. The analysis was done using FEM. Thickness of the partition was varied to visualize the effect of Re on streamline and temperature. The variation of average Nusselt number with both Reynolds and Grashof numbers was observed ,

2. Literature Review

There are several numbers of authors who paid attention to mixed convection in a cavity . Reyad Omari [4] investigated constant laminar mixed convection flow and heat transfer in a lid-driven cavity using CFD simulation. He discovered that the aspect ratio and Reynolds number have a large influence on the average Nusselt number inside the cavity, and that decreasing the aspect ratio or increasing the Reynolds number improved heat transfer. In a differentially heated partitioned enclosure, Mahpatra et al. [5] examined opposing mixed convection. They discovered that when the height of a centrally situated partition exceeds $0.3H$, the heat transfer in the case of opposing mixed convection for a partitioned enclosure is greater than that of natural convection. Over a variety of Richardson numbers, Yapici et al. [6] investigated steady laminar mixed-convection heat transfer in a two-dimensional square lid-driven chamber with a modified heated wall. They came to the conclusion that heat transfer enhancement is often noticed with the change of the heated wall, with the improvement being more significant in the case of rectangular waves and

low Richardson numbers. Saha et al.[7] studied a problem of partitioned vertical cavity for conjugate natural convection into air and water regions. They found that corrugation amplitude, thermal conductivity, position and thickness of the partition are the controlling parameters that effects the overall thermal performance. Among them increasing partition thickness it is found that increasing partition thermal conductivity enhances thermal performance by up to 25%. Oztop et al.[8] studied a similar mixed convection problem for varying Richardson number by maintaining the thickness of the partitioned wall constant. They observed that higher heat transfer was formed for higher Richardson number for upward moving wall for all values of thermal conductivity ratio. Saha et al. [9] observed laminar, steady, incompressible mixed convection for a double lid driven cavity. They considered both hot and cold walls moving. They observed that a change in Re causes major changes in the average Nu. They also observed that the increment of Re results in the formation of boundary layers on the heated wall of the cavity, where the velocity over the cavity decreases. Pal et al. [10] studied FEM analysis of laminar, steady, incompressible mixed convection for a double lid driven cavity, where 2 cold walls were moving. They observed that heat transfer decreases with the increase of Ri, whereas it increases with the increase of Pr. They also showed that the effect of Re is dominated by forced convection. Ahmed [11] studied FEM analysis of two-dimensional mixed convection of nanofluid in a square cavity with a circular body in it. He observed that with the increase of Re, Nu increases as well. For partitioned cavity with variable thickness of partition, in previous studies, no moving lid was considered. Studies that considered moving lid, didn't consider variable thickness of partition. In this study, both moving lid and variable thickness of partition was considered. The effect of changing partition thickness was shown briefly with streamline and temperature plot.

3. Methods

3.1 Physical Model

Figure 1 shows a two-dimensional differentially heated square enclosure of length L , vertically partitioned by a heat conducting solid wall of thickness t_p and thermal conductivity k_s in Cartesian coordinate system. In this study, both top and bottom walls of the enclosure are assumed to be adiabatic, while the vertical side walls are kept at constant temperature T_h and T_c ($T_h > T_c$), respectively. The solid partition is placed vertically at $x = x_p$ position inside the enclosure, which separates the whole computational domain into two convection regions filled with two types of working fluid, and one conduction region within the partition wall of the enclosure. The working fluid in the left and the right convective domains are considered as water and air respectively. Epoxy is chosen as the partition material of the enclosure. In the present investigation, the thickness and the position of the solid partition from the hot wall are varied to assess the heat transfer performance of the partitioned enclosure.

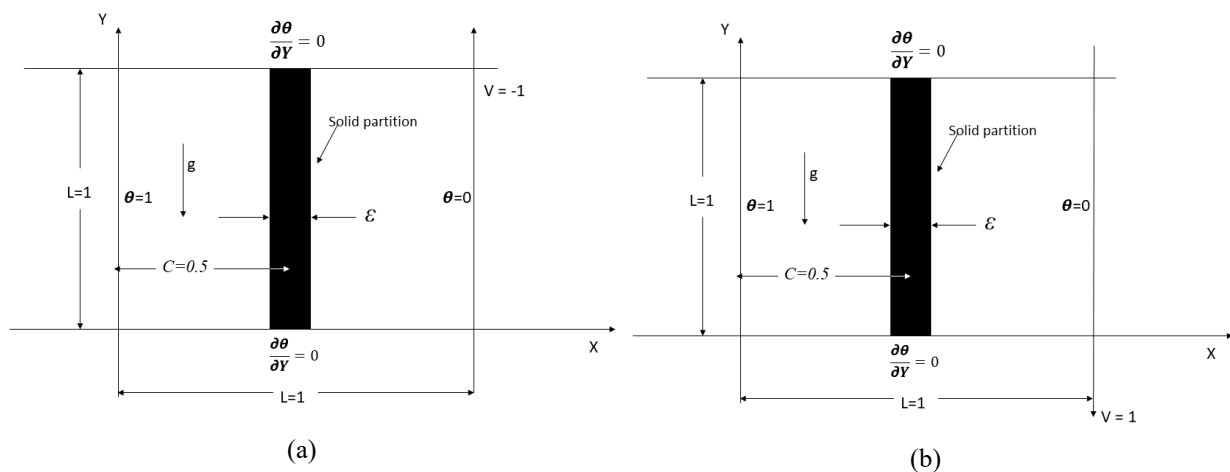


Fig.1. Schematic diagram of the partitioned enclosure along with boundary conditions for (a) upward lid direction, (b) downward lid direction

Partition material: SS Steel 302, $k_s = 15.1 \frac{W}{mK}$ @300K

Air, $k_a = 0.02624 \frac{W}{mK}$ @25°C, Pr = 0.708

3.2 Mathematical Model

The flow inside the enclosure is considered to be steady state, two-dimensional, laminar and incompressible. The thermophysical properties of both working fluids are considered to be constant except the temperature dependent density variation in the body force as expressed by Boussinesq approximation. Any viscous dissipation and radiation effect within the enclosure are neglected and there is no internal heat generation. Under the above considerations, the mass, momentum and energy equations in Cartesian coordinate system are given as follows:

For air domain:

$$\frac{\partial u}{\partial x} + \frac{\partial v}{\partial y} = 0, \quad (1)$$

$$\rho_a \left(u \frac{\partial u}{\partial x} + v \frac{\partial u}{\partial y} \right) = -\frac{\partial p}{\partial x} + \mu_a \left(\frac{\partial^2 u}{\partial x^2} + \frac{\partial^2 u}{\partial y^2} \right), \quad (2)$$

$$\rho_a \left(u \frac{\partial v}{\partial x} + v \frac{\partial v}{\partial y} \right) = -\frac{\partial p}{\partial y} + \mu_a \left(\frac{\partial^2 v}{\partial x^2} + \frac{\partial^2 v}{\partial y^2} \right) + \rho_a g \beta_a (T - T_c), \quad (3)$$

$$\rho_a C_{p,a} \left(u \frac{\partial T}{\partial x} + v \frac{\partial T}{\partial y} \right) = k_a \left(\frac{\partial^2 T}{\partial x^2} + \frac{\partial^2 T}{\partial y^2} \right), \quad (4)$$

For solid domain:

$$k_s \left(\frac{\partial^2 T}{\partial x^2} + \frac{\partial^2 T}{\partial y^2} \right) = 0, \quad (5)$$

where, x and y are the Cartesian coordinates, u and v are the velocity components in the x - and y - directions respectively, p is the pressure, T is the temperature and g is the gravitational acceleration. The thermophysical properties such as density, dynamic viscosity, thermal conductivity, specific heat at constant pressure and thermal expansion coefficient are expressed as ρ , μ , k , C_p and β respectively. The subscripts 'a', 'w' and 's' represent the properties of air, water and solid material respectively.

In order to obtain non-dimensional governing equation in pressure-velocity formulation, the following dimensionless variables are employed:

$$X = \frac{x}{L}, Y = \frac{y}{L}, U = \frac{u}{u_0}, V = \frac{v}{u_0}, P = \frac{p}{\rho u_0^2}, \Theta = \frac{T - T_c}{T_h - T_c}, \alpha_a = \frac{k_a}{\rho_a C_{p,a}} \quad (6)$$

where, X and Y are the non-dimensional Cartesian coordinates, U and V are the non-dimensional velocity components in the X and Y -directions respectively P and Θ are the non-dimensional pressure and the non-dimensional temperature respectively, and α is the thermal diffusivity. Using the above scales (6), the dimensional governing equations (1) – (9) can be transformed to a set of non-dimensional equations as follows:

For air domain:

$$\frac{\partial U}{\partial X} + \frac{\partial V}{\partial Y} = 0, \quad (7)$$

$$U \frac{\partial U}{\partial X} + V \frac{\partial U}{\partial Y} = -\frac{\partial P}{\partial X} + \frac{1}{Re} \left(\frac{\partial^2 U}{\partial X^2} + \frac{\partial^2 U}{\partial Y^2} \right) \quad (8)$$

$$U \frac{\partial V}{\partial X} + V \frac{\partial V}{\partial Y} = -\frac{\partial P}{\partial Y} + \frac{1}{Re} \left(\frac{\partial^2 V}{\partial X^2} + \frac{\partial^2 V}{\partial Y^2} \right) \quad (9)$$

$$U \frac{\partial \Theta}{\partial X} + V \frac{\partial \Theta}{\partial Y} = \frac{1}{RePr} \left(\frac{\partial^2 \Theta}{\partial X^2} + \frac{\partial^2 \Theta}{\partial Y^2} \right) \quad (10)$$

For solid domain:

$$\frac{1}{RePr} \frac{k_s}{k_a} \left(\frac{\partial^2 \Theta}{\partial X^2} + \frac{\partial^2 \Theta}{\partial Y^2} \right) = 0 \quad (11)$$

where, Gr_a and Pr_a are Grashof and Prandtl numbers of air respectively. For water domain, these two governing parameters can also be expressed as Gr_w and Pr_w respectively. All these non-dimensional parameters are defined by following relations:

$$Re = \frac{\rho_a u_0 L}{\mu_a}, Gr = \frac{\rho_a^2 g \beta_a (T_h - T_c) L^3}{\mu_a^2}, Pr = \frac{C_{p,a} \mu_a}{k_a}, Ri = \frac{Gr}{Re^2} \quad (12)$$

The thermophysical properties of the working fluid (air and water) and the partition material (epoxy) evaluated at 298K [1] are listed in Table 1.

Table 1: List of thermophysical properties of working fluids and partition material at 300K.

Properties	Air	SS Steel 302
k (W/m.K)	0.02624	15.1
Pr	0.708	

For all solid surfaces (enclosure walls and partition), no-slip conditions are imposed on those boundaries. Since the solid partition is a heat conducting material, the solid-fluid interface follows a continuity boundary condition. The list of flow and thermal boundary conditions for all boundaries in non-dimensional form is presented in Table 2.

Table 2: Non-dimensional boundary conditions for the present problem.

Dependent variables	Left wall	Right wall	Top and bottom walls	Partition walls	
				Left side	Right side
Velocity	$U = V = 0$	$U = 0$ $V = -1$ (downward moving) $V = 1$ (upward moving)	$U = V = 0$	$U = V = 0$	$U = V = 0$
Temperature	$\Theta = 1$	$\Theta = 0$	$\frac{\partial \Theta}{\partial Y} = 0$	$k_a \left(\frac{\partial T}{\partial x} \right)_a = k_s \left(\frac{\partial T}{\partial x} \right)_s$ $\left(\frac{\partial \Theta}{\partial X} \right)_a = \frac{k_s}{k_a} \left(\frac{\partial \Theta}{\partial X} \right)_s$	

Table 3: Selection of governing and geometric parameters used in the present simulation.

Parameter	Values of interest
Richardson number, Ri	1 (pure MC)
Reynolds number, Re	$1 \leq Re \leq 1000$
Non-dimensional partition position, $c = \frac{x_p}{L}$	0.50
Non-dimensional partition thickness, $\varepsilon = \frac{t_p}{L}$	0.05, 0.10, 0.20
Prandtl number of air, Pr_a	0.708
Ratio of thermal conductivity, $\frac{k_s}{k_a}$	575.4573

Thermal performance of the enclosure is evaluated in terms of average Nusselt number of the hot wall which is defined as follows:

$$Nu_H = \frac{h_H L}{k_a} = - \int_0^1 \frac{\partial \theta}{\partial X} \Big|_{x=1} dY \quad (13)$$

where h_H is the hot wall's average convection heat transfer coefficient. Furthermore, the thermal performance of the partition is measured in terms of the average Nusselt number of the partition's left and right sides, which are defined as follows:

$$Nu_{LSP} = \frac{h_{LSP} L}{k_a} = - \frac{\int_0^1 \frac{\partial \theta}{\partial X} \Big|_{x=c-\frac{\varepsilon}{2}} dY}{\int_0^1 \theta \Big|_{x=c-\frac{\varepsilon}{2}} dY} \quad (14)$$

$$Nu_{RSP} = \frac{h_{RSP} L}{k_a} = - \frac{\int_0^1 \frac{\partial \theta}{\partial X} \Big|_{x=c+\frac{\varepsilon}{2}} dY}{\int_0^1 \theta \Big|_{x=c+\frac{\varepsilon}{2}} dY} \quad (15)$$

where, h_{LSP} and h_{RSP} are the average convection heat transfer coefficients of the left and the right sides of the partition wall respectively, $c = \frac{x_p}{L}$ is the non-dimensional partition position from the hot wall and $e_p = \frac{t_p}{L}$ is the non-dimensional partition thickness. For conjugate natural convection heat transfer within the partitioned enclosure, a measure of overall thermal performance of the partitioned enclosure is essential to assess the influence of

the governing parameters. Hence, a ratio of overall heat transfer coefficient (U_o) to average convection heat transfer coefficient along the hot wall is expressed by the following relation:

$$\frac{U_o}{h_H} = \frac{1}{\frac{Nu_H}{Nu_{LSP}} + \varepsilon \frac{k_a}{k_s} Nu_H + \frac{Nu_H}{Nu_{RSP}}} \quad (16)$$

4. Results and Discussion

Case a : Upward moving lid direction(Cold wall)

4.1 Effect of Partition thickness on streamlines

The characteristics of flow in the enclosure for Case I (upward moving right wall) are shown in Fig 2 for partition thickness , $ep=0.05$ and different Reynolds numbers ($Re= 1,10,20,50,70,100,150,200$) via streamlines .Effect of partition thickness on streamlines was investigated by changing partition thickness ($ep = 0.1$ in Fig 3 and $ep=0.2$ in Fig 4). It is observed that the direction of streamlines is in anti-clockwise for upward moving right wall . Also, for a same partition thickness , vortex is formed with the increase of Re number. And ,when we increased Partition thickness , it is found that the vortex generation started occurring for a small Re number.

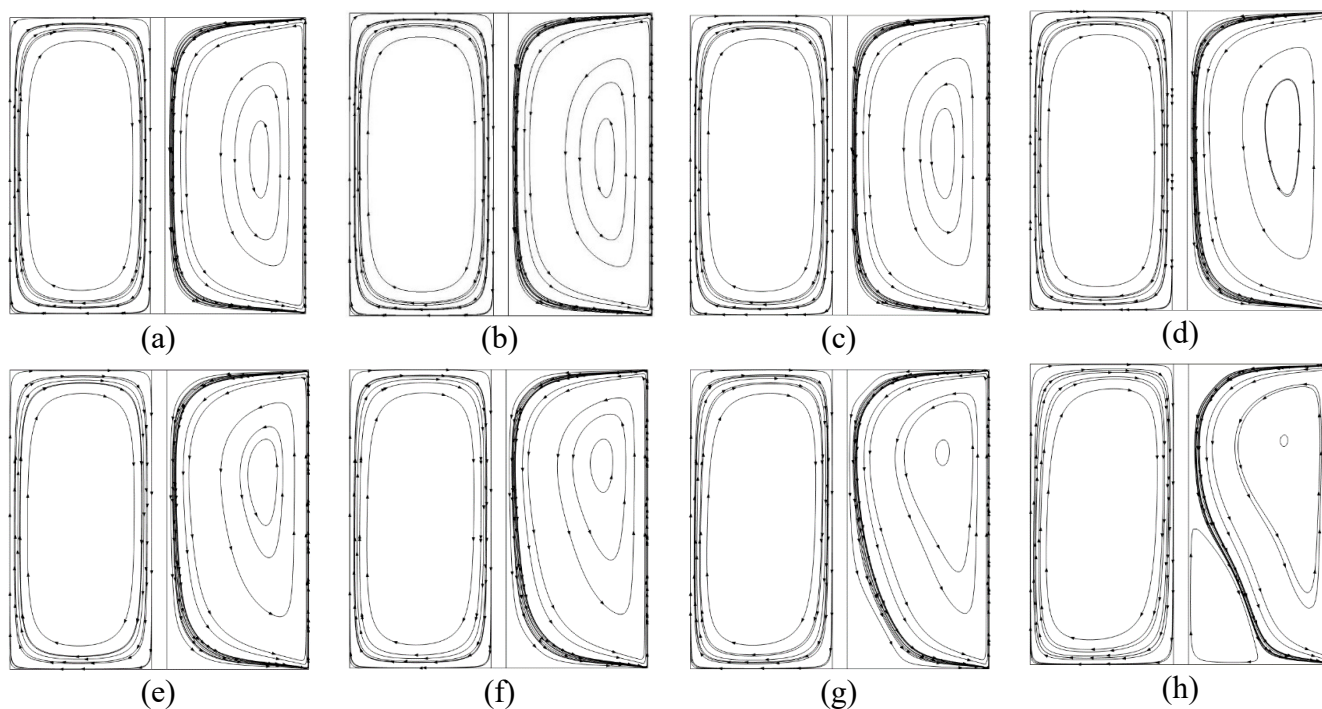


Figure 2 : Streamline plot for $ep=0.05$ and a) $Re=1$, b) $Re=10$, c) $Re=20$, d) $Re=50$, e) $Re=70$, f) $Re=100$, g) $Re=150$, h) $Re=200$

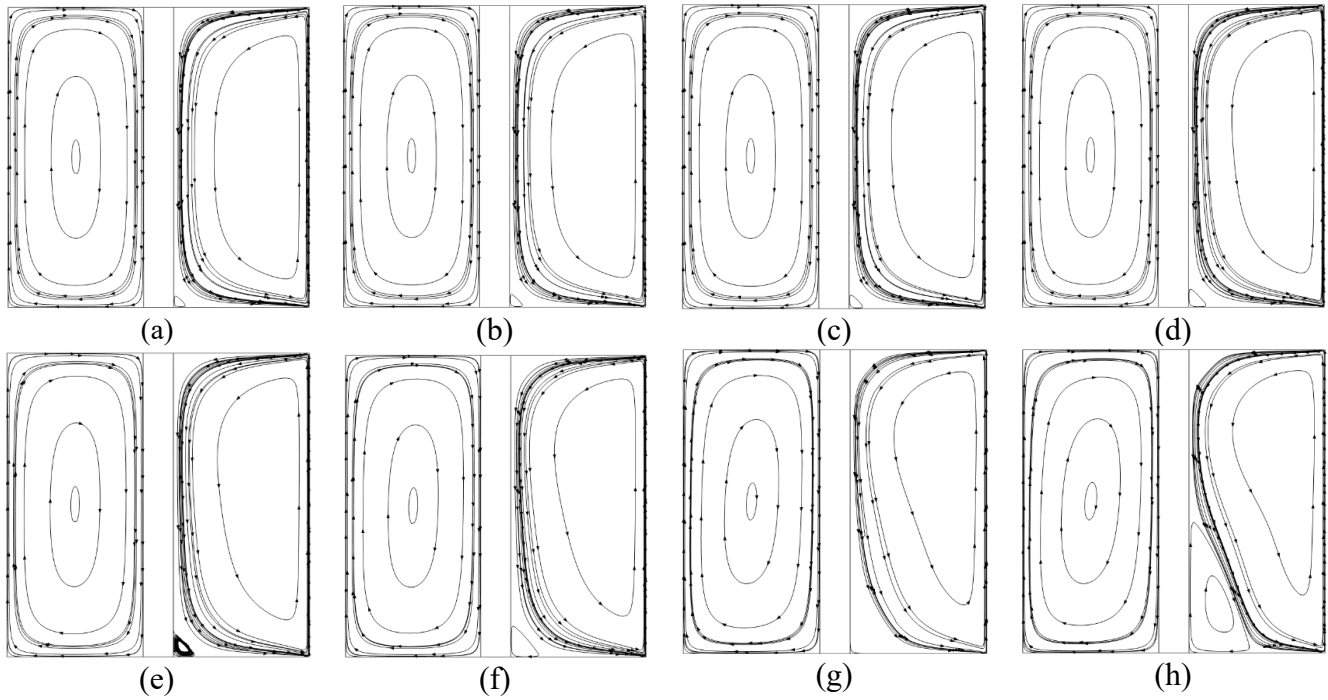


Figure 3 : Streamline plot for $ep=0.1$ and a) $Re=1$, b) $Re=10$, c) $Re=20$, d) $Re=50$, e) $Re=70$, f) $Re=100$, g) $Re=150$, h) $Re=200$

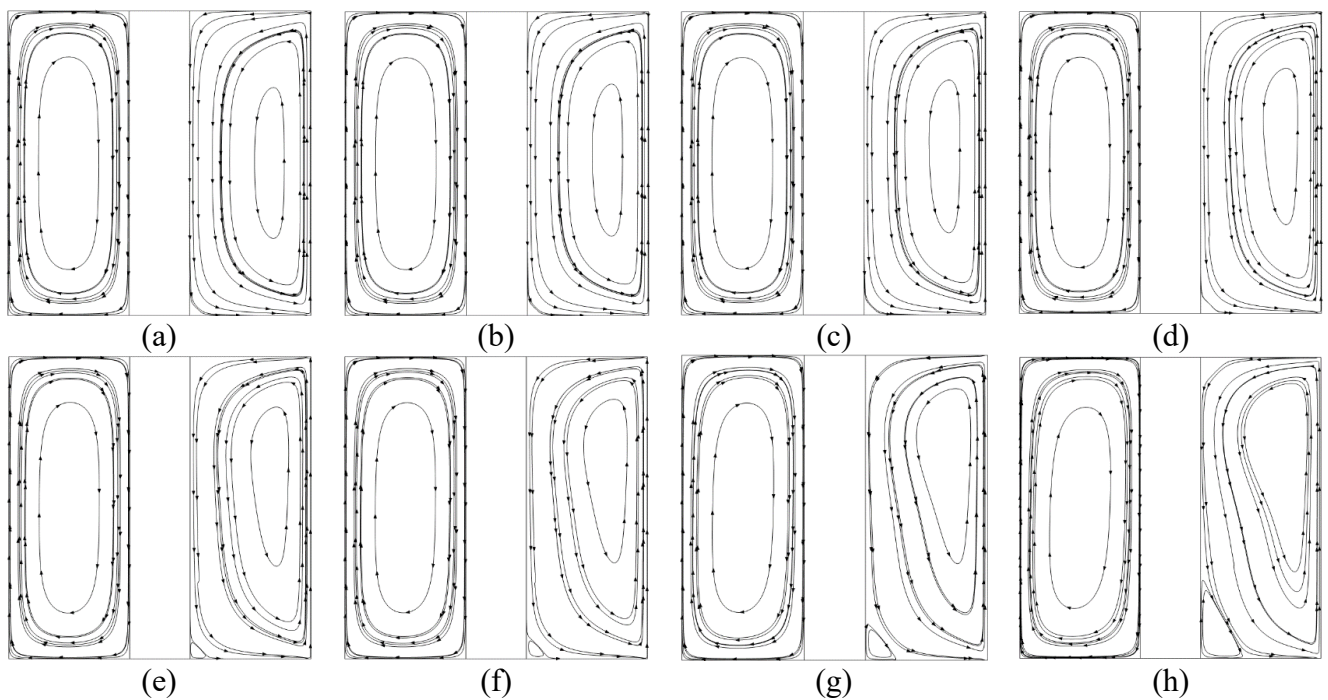


Figure 4 : Streamline plot for $ep=0.2$ and a) $Re=1$, b) $Re=10$, c) $Re=20$, d) $Re=50$, e) $Re=70$, f) $Re=100$, g) $Re=150$, h) $Re=200$

4.2 Effect of Partition thickness on temperature contour

According to Fig 5, Fig 6, Fig 7; At lower Reynolds number and lower partition thickness, the isotherm lines are parallel to the wall as expected. Regardless of the variation in partition thickness, linear temperature profiles (due to conduction) continue to progress inside the solid partition wall. When looking at the value of the isotherm label, it is evident that conduction heat transfer in the cavity improves over convection as the thickness of the partition wall increases. As Re number increased ($Re > 20$), distorted isotherms are observed. At $Re \geq 70$ distorted isotherms are observed in both the sides of the partition. Distorted isotherm lines indicate higher heat transfer. When looking at the value of the isotherm label, it is evident that conduction heat transmission improves as the thickness of the partition wall increases.

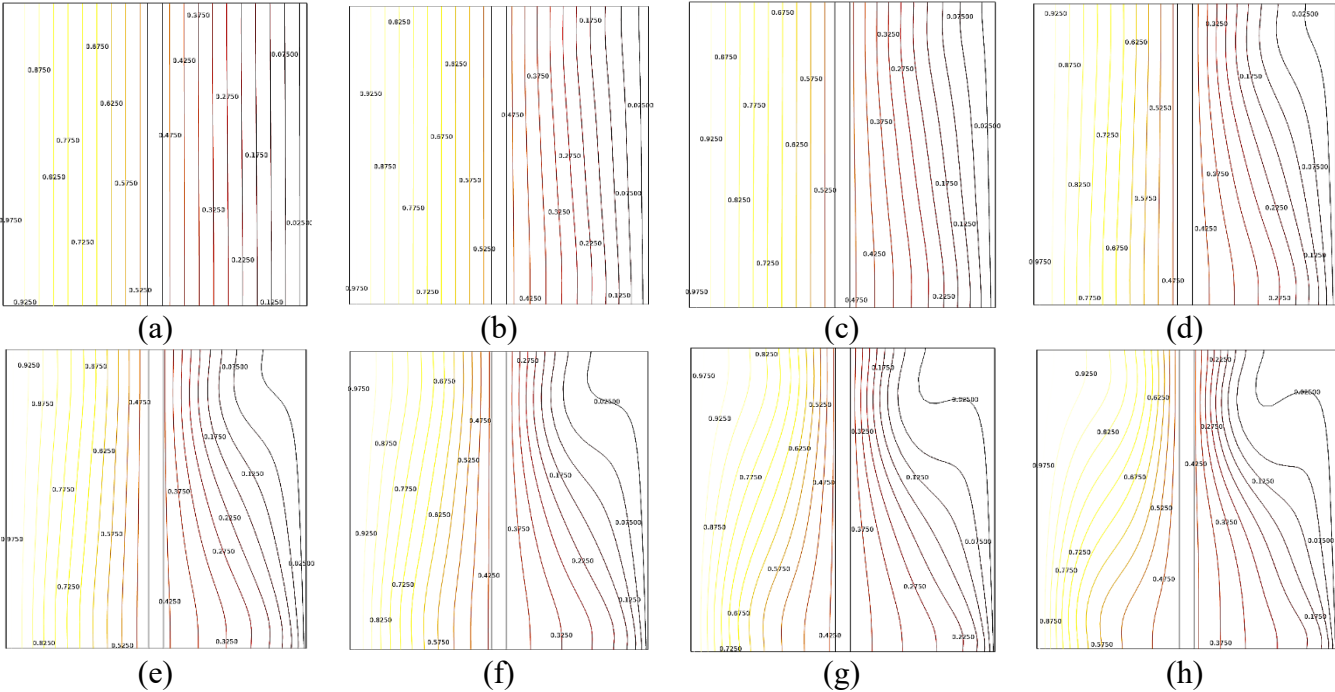
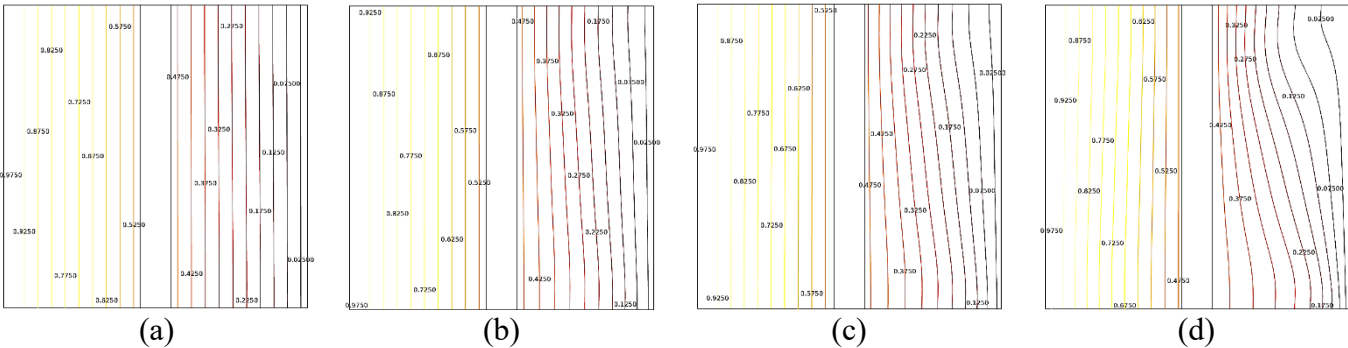


Figure 5: Temperature Contours for $ep=0.05$ and a) $Re=1$, b) $Re=10$, c) $Re=20$, d) $Re=50$, e) $Re=70$, f) $Re=100$, g) $Re=150$, h) $Re=200$



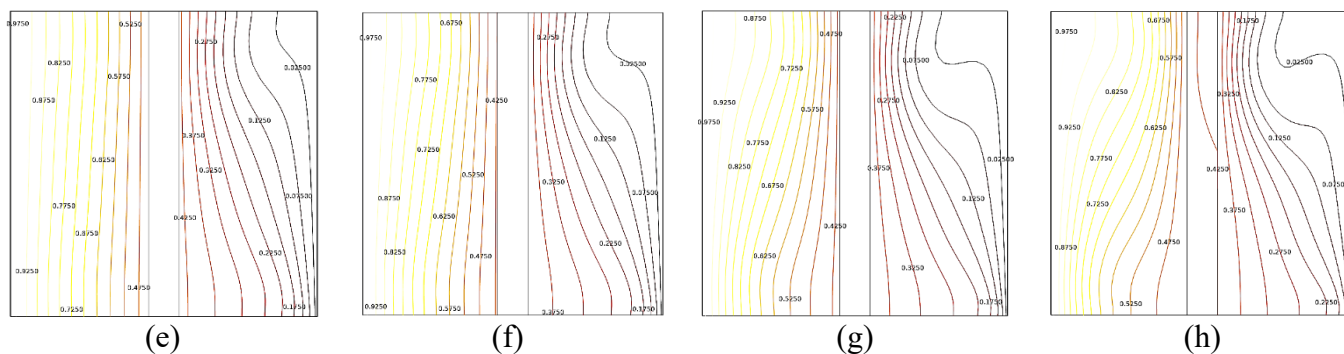


Figure 6: Temperature Contours for $ep=0.1$ and a) $Re=1$, b) $Re=10$, c) $Re=20$, d) $Re=50$, e) $Re=70$, f) $Re=100$, g) $Re=150$, h) $Re=200$

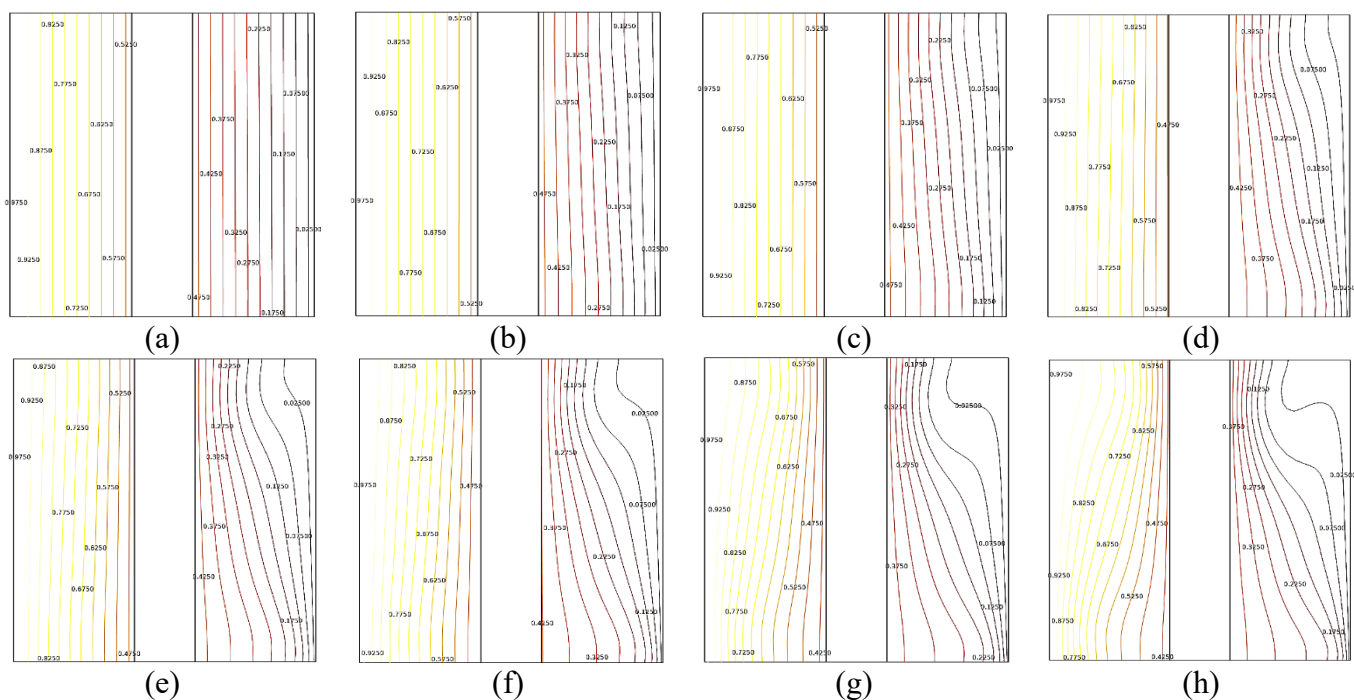


Figure 7: Temperature Contours for $ep=0.2$ and a) $Re=1$, b) $Re=10$, c) $Re=20$, d) $Re=50$, e) $Re=70$, f) $Re=100$, g) $Re=150$, h) $Re=200$

4.3 Variation of Nusselt number with the change of Reynolds Number and partition thickness for upward moving right wall

It is observed from the Fig 8 that Nusselt number is increasing with the increasing of Reynolds number. But for the same Reynolds number Nusselt number increases with increasing the partition thickness. Nusselt number is the representation of the method of heat transfer. If the Nusselt number is high, it means that the heat transfer by conduction is the dominant method than convection. So, greater partition thickness causes more conduction in the cavity.

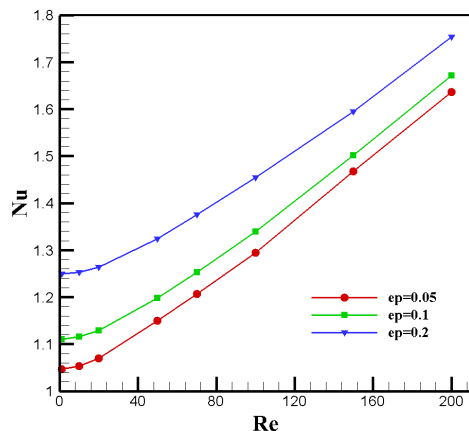


Figure 8: Variation of Nu with the change of Re in different thickness of partition for upward moving right wall

Case b : Downward moving lid (cold wall)

4.4 Effect of Partition thickness on streamlines

The features of flow in the enclosure for Case 2 (downward moving right wall) are also illustrated in Fig 9 for partition thicknesses=0.05, and various Reynolds numbers (Re= 1,10,20,50,70,100,150,200) through streamlines . Similarly, to case 1, the influence of partition thickness on streamlines was explored for case 2 by adjusting partition thicknesses (ep = 0.1 in Fig 10 and ep=0.2 in Fig 11). The direction of streamlines for the upward advancing right wall is seen to be anticlockwise in this example. Additionally, when the Re number is increased, vortex is created for the same partition thickness. And, as the partition thickness was increased, the vortex production began to occur for a small Re number.

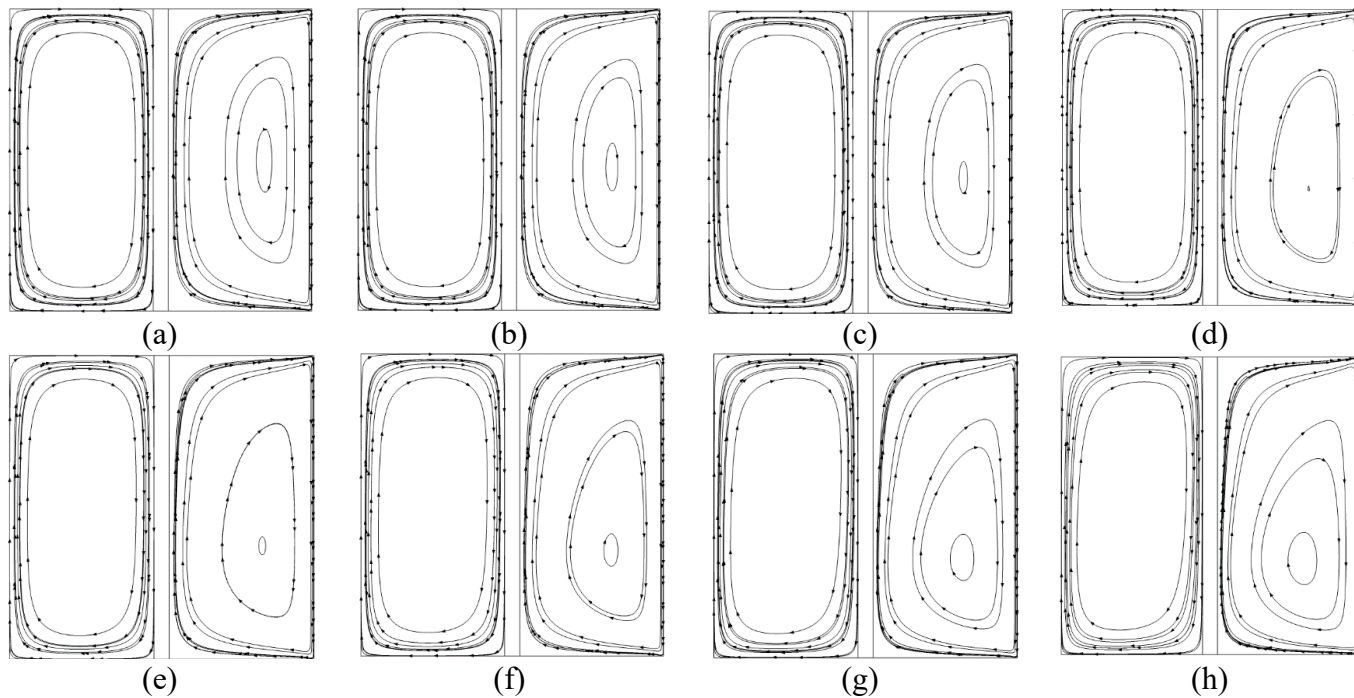


Figure 9: Streamline plot for ep=0.05 and a) Re=1, b)Re=10, c)Re=20, d)Re=50, e)Re=70, f)Re=100, g)Re=150, h)Re=200

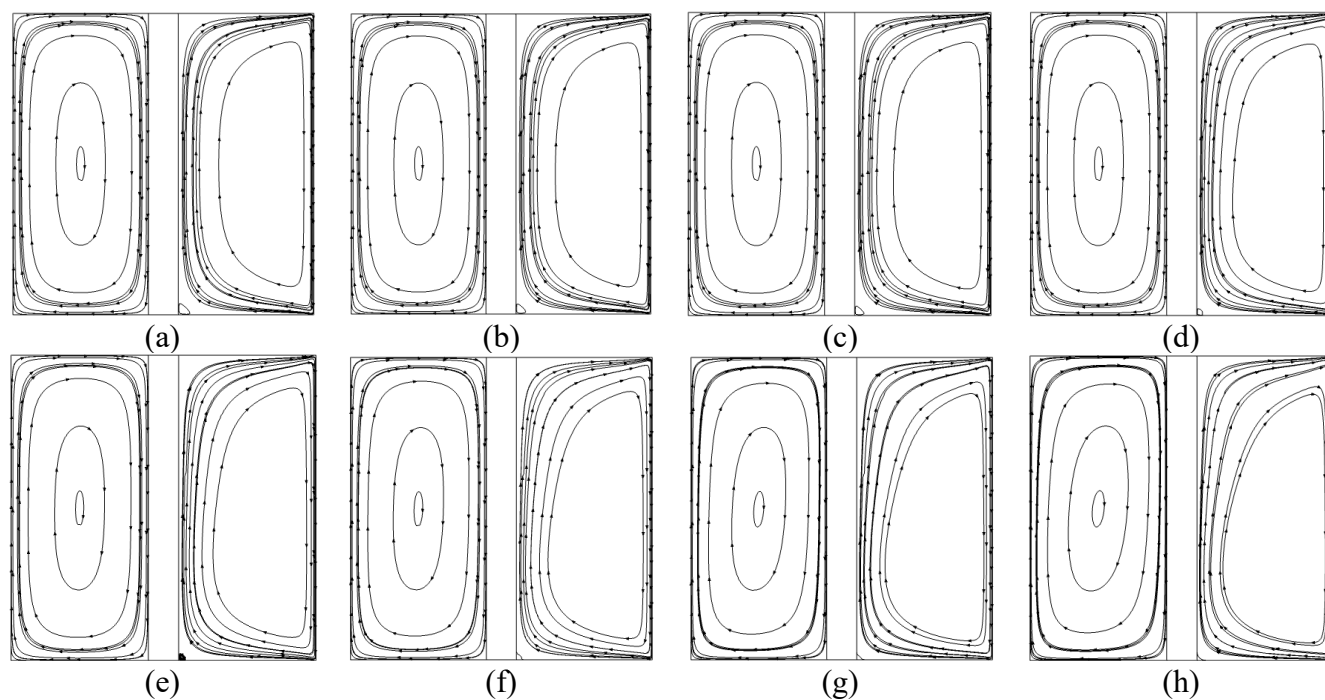


Figure 10: Streamline plot for $ep=0.1$ and a) $Re=1$, b) $Re=10$, c) $Re=20$, d) $Re=50$, e) $Re=70$, f) $Re=100$, g) $Re=150$, h) $Re=200$

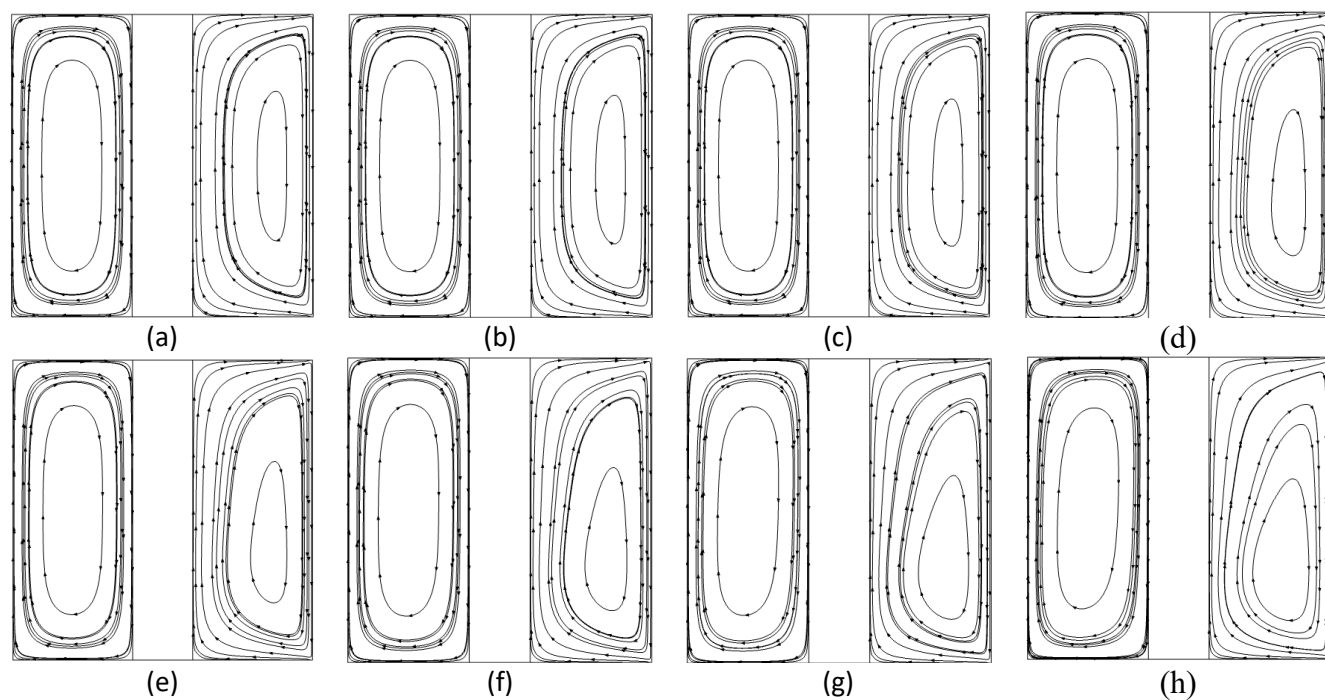


Figure 11: Streamline plot for $ep=0.2$ and a) $Re=1$, b) $Re=10$, c) $Re=20$, d) $Re=50$, e) $Re=70$, f) $Re=100$, g) $Re=150$, h) $Re=200$

4.5 Effect of Partition thickness on temperature contour

A similar result like the upward moving wall was observed for the downward moving wall (Fig: 12 .Fig 13 and Fig 14) But the concave part of the distorted isotherms is placed downward as expected. At higher Reynolds number the more heat transfer occurs as usual.

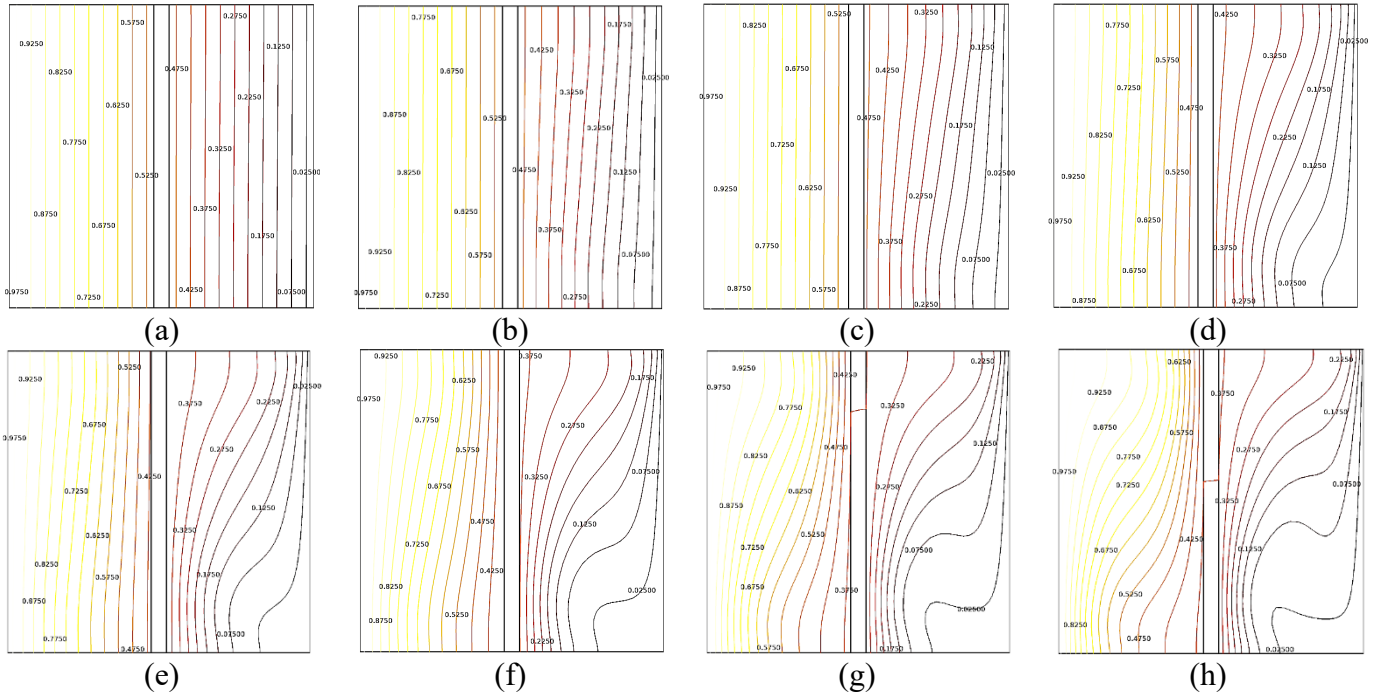


Figure 12: Temperature Contours for $ep=0.05$ and a) $Re=1$, b) $Re=10$, c) $Re=20$, d) $Re=50$, e) $Re=70$, f) $Re=100$, g) $Re=150$, h) $Re=200$

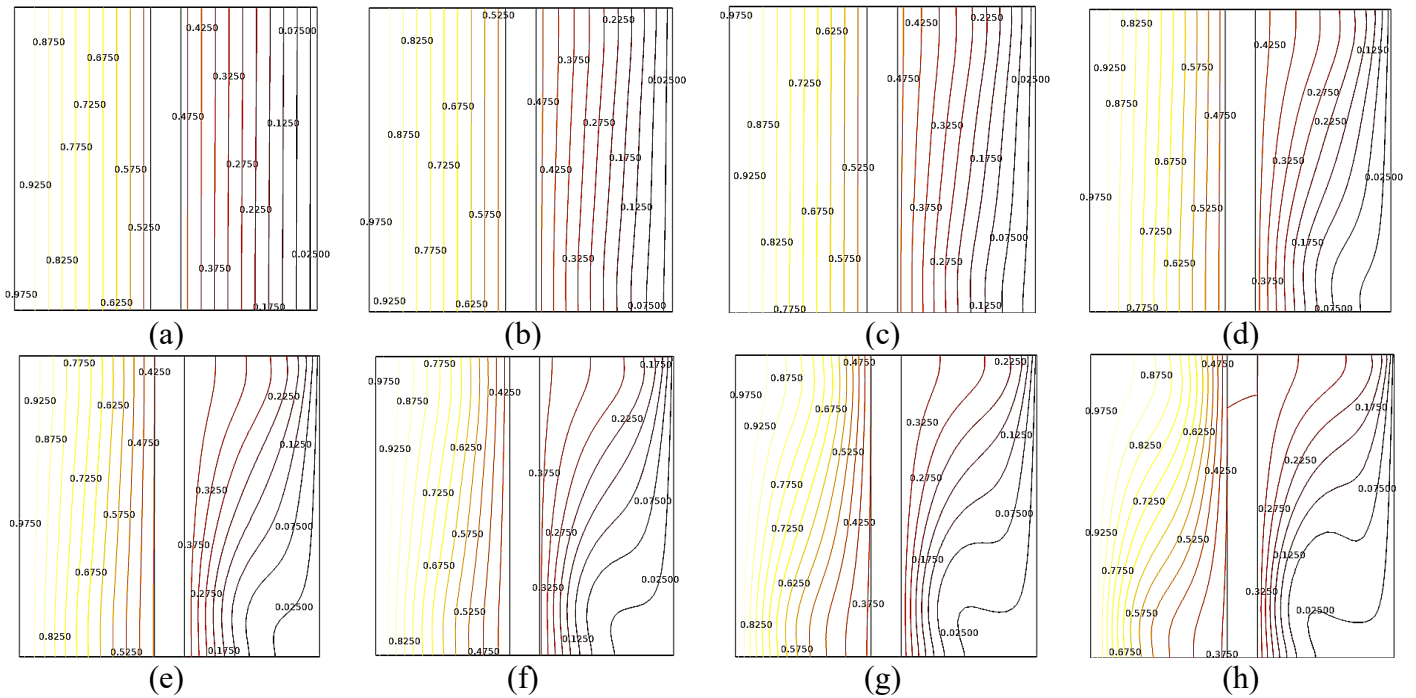


Figure 13: Temperature Contours for $ep=0.1$ and a) $Re=1$, b) $Re=10$, c) $Re=20$, d) $Re=50$, e) $Re=70$, f) $Re=100$, g) $Re=100$, h) $Re=100$

g)Re=150, h)Re=200

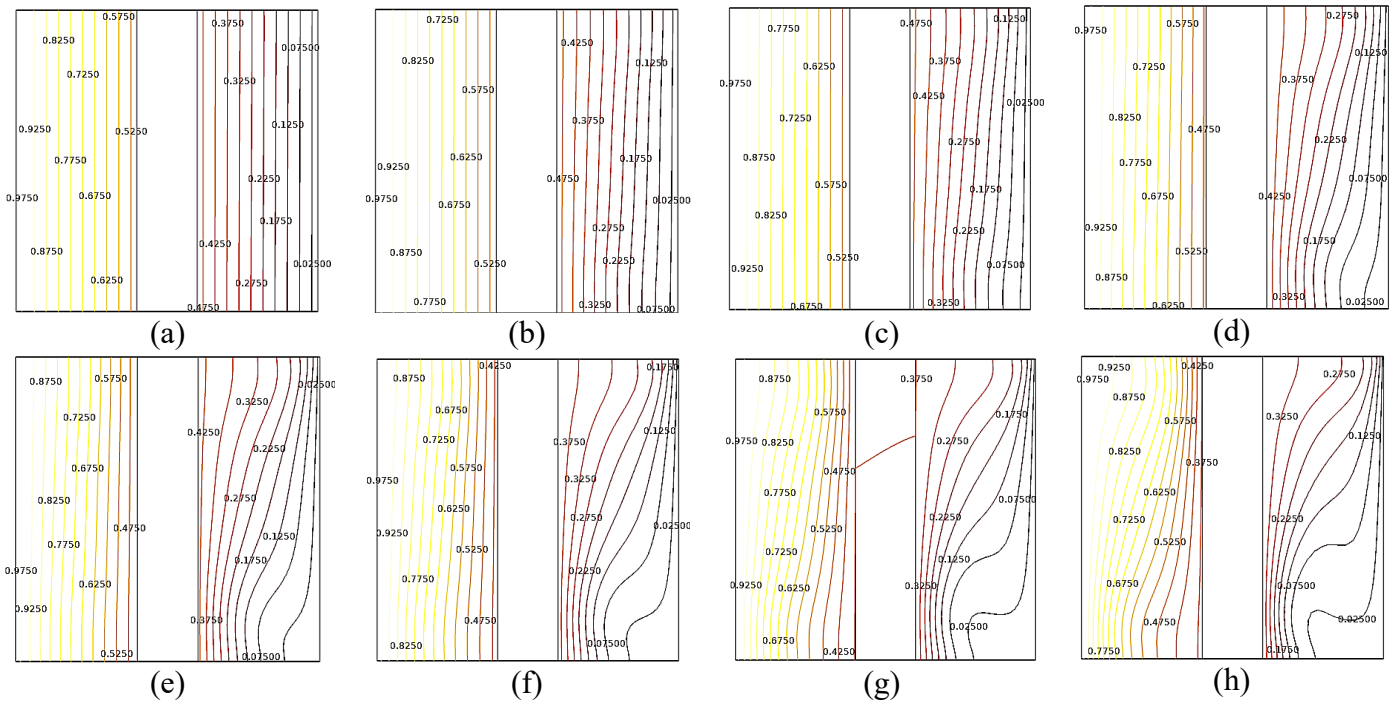


Figure 14: Temperature Contours for $ep=0.2$ and a) $Re=1$, b) $Re=10$, c) $Re=20$, d) $Re=50$, e) $Re=70$, f) $Re=100$, g) $Re=150$, h) $Re=200$

4.6 Variation of Nusselt number with the change of Reynold Number and partition thickness for downward moving right wall

Almost same result for downward moving right wall is also observed as the upward moving wall. But from Fig 15 it is observed that at partition thickness 0.05 and 0.1 mm the Nusselt number is almost similar at Reynolds number 200.

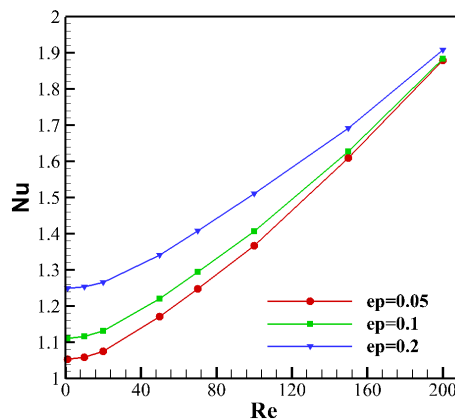


Figure 15: Variation of Nu with the change of Re in different thickness of partition for downward moving right wall

4.7 Calculation of overall thermal performance coefficient and effect of Reynolds number and partition thickness on overall thermal performance coefficient for both upward and downward moving right wall

Overall thermal performance coefficient was calculated in this work using equation (16). Calculation was done using COMSOL Multiphysics. Fig [16] shows the plot of overall thermal performance coefficient vs Reynolds number in three different partition thickness for upward moving right or cold wall. Fig[17] shows the same but in this case, it is for downward moving lid. From both the figure it is visible that for lower Re overall thermal performance coefficient increases with increase of Re. But after a certain value of Re it decreases with the increase of Re.

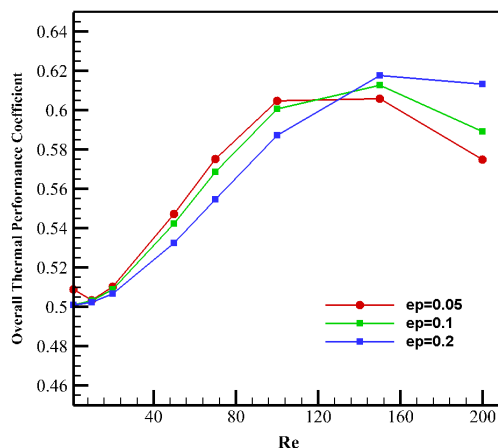


Fig 16 : Variation of overall thermal performance coefficient with the change of Re for different thickness for upward moving right wall

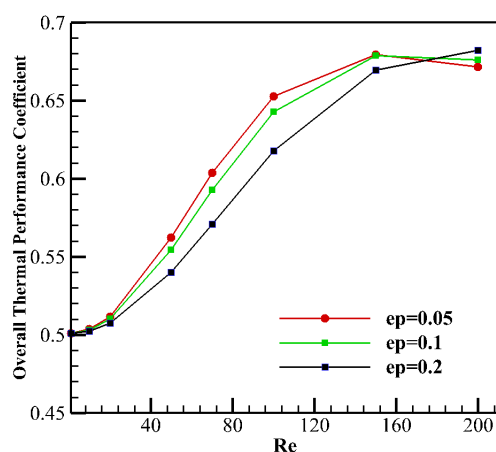


Fig 17 : Variation of overall thermal performance coefficient with the change of Re for different thickness for downward moving right wall

4.8 Validation

To compare the reported results to the literature, we conducted one validation test. The computational technique is validated against T.S. Cheng [13] 's results for characteristics of mixed convection heat transfer in a lid driven square cavity with various Richardson and Prandtl numbers. The general agreement between this computation and that of T.S. Cheng is quite good. Figure[17] shows the plot of the Nusselt number (along the bottom wall) vs Reynolds number while Richardson number kept fixed constant at 0.01. It is seen that both the plot (Ts Cheng's and present model) is almost similar.

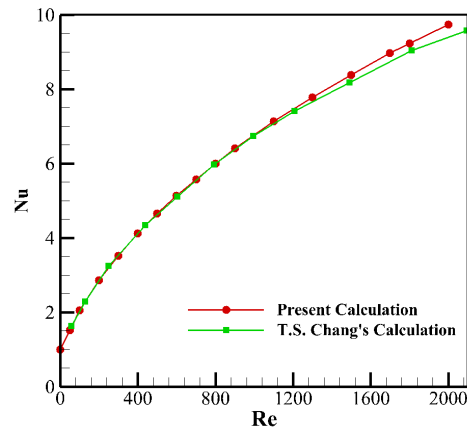


Fig 18: Comparison of average Nusselt number along the bottom wall obtained by the present model with that of T.S. Cheng [13]

5. Conclusion

This research looked at the effect of Reynolds number and partition thickness for the flow inside a lid driven square cavity on conjugate mixed convection in the presence of adiabatic horizontal walls. As described in mathematical model section, the Equations (7-11) were solved using FEM method. The investigation has been performed for Reynolds number 1 to 200. It's worth noting that the Richardson (Ri) is kept constant at $Ri=1$. The following conclusions can be drawn from the current research:

1. Nusselt number increases with the increase of Reynold number for a particular thickness
2. Nusselt number increases with the increase in partition thickness
3. Temperature contours shifts from linear to nonlinear with the increase of Reynolds number
4. When the Re number is increased, vortex is created for the same partition thickness
5. As the partition thickness was increased, the vortex production began to occur for a small Re number.

Acknowledgements

We would express our profound gratitude to the Computational Fluid Dynamics and Heat Transfer (CFDHT) Research Group of Department of Mechanical Engineering, Bangladesh University of Engineering and Technology (BUET) for providing continuous support throughout our research works.

References

- [1] S. Bilir, A. Ates, Transient conjugated heat transfer in thick walled pipes with convective boundary conditions, *Int. J. Heat Mass Transfer* 46 (2003) 2701–2709.
- [2] E. Papanicolaou, Y. Jaluria, Mixed convection from simulated electronic components at varying relative positions in a cavity, *J. Heat Transfer* 116 (1994) 960–970.
- [3] E. Papanicolaou, Y. Jaluria, Mixed convection from a localized heat source in a cavity with conducting walls, *Numer. Heat Transf. A Appl.* 23 (1993) 463–484.
- [4] Omari, R. (2016) Numerical Investigation of a Mixed Convection Flow in a Lid-Driven Cavity. *American Journal of Computational Mathematics*, 6, 251-258.
- [5] S.K. Mahapatra, Anjan Sarkar, A. Sarkar, Numerical simulation of opposing mixed convection in differentially heated square enclosure with partition, *International Journal of Thermal Sciences*, Volume 46, Issue 10, 2007, Pages 970-979, ISSN 1290-0729,
- [6] Kerim Yapici & Salih Obut (2015) Laminar Mixed-Convection Heat Transfer in a Lid-Driven Cavity with Modified Heated Wall, *Heat Transfer Engineering*, 36:3, 303-314
- [7] Shadman Sakib Priam, Maruf Md. Ikram, Sumon Saha, Suvash C. Saha, Conjugate natural convection in a vertically divided square enclosure by a corrugated solid partition into air and water regions, *Thermal Science and Engineering Progress*, Volume 25, 2021, 101036, ISSN 2451-9049

- [8] Hakan F. Oztop, Zepu Zhao, Bo Yu, Conduction-combined forced and natural convection in lid-driven enclosures divided by a vertical solid partition, *International Communications in Heat and Mass Transfer*, Volume 36, Issue 7, 2009, Pages 661-668, ISSN 0735-1933.
- [9] Saha, Kajal Chandra, Goutam Saha, and Doli Rani Pal. "Double Lid Driven Cavity with Different Moving Wall Directions for Low Reynolds Number Flow." *International Journal of Applied Mathematics and Theoretical Physics* 4.3 (2018): 67.
- [10] Pal, Doli Rani, Goutam Saha, and Kajal Chandra Saha. "A case study of double lid driven cavity for low Reynolds number flow." *Dhaka University Journal of Science* 66.2 (2018): 95-101.
- [11] Ahmed, Adnan. *MHD Mixed Convection Nanofluid Flow and Heat Transfer in a Cavity with Circular Cylinder*. Diss. CAPITAL UNIVERSITY, 2019.
- [12] Cengel, Y. and Ghajar, A. (2015). *Heat and mass transfer: fundamentals and applications*. McGraw-Hill Education; 5th edition.
- [13] T.S. Cheng, Characteristics of mixed convection heat transfer in a lid-driven square cavity with various Richardson and Prandtl numbers, *International Journal of Thermal Sciences*, Volume 50, Issue 2, 2011, Pages 197-205, ISSN 1290-0729,

Biographies

Mir Atiqur is pursuing B.Sc. in Mechanical Engineering from Bangladesh University of Engineering and Technology (BUET). His research interest is focused to computational heat transfer, CFD, molecular dynamics, automobile.

Md Alif Mahmud is pursuing B.Sc. in Mechanical Engineering from Bangladesh University of Engineering and Technology (BUET). His research interest is focused to computational heat transfer, CFD, molecular dynamics, heat engine.

R. K. B. M. Rizmi is pursuing B.Sc. in Mechanical Engineering from Bangladesh University of Engineering and Technology (BUET). His research interest is focused to computational heat transfer, CFD, molecular dynamics, mechatronics.

Dr. Sumon Saha received his PhD in Engineering from the University of Melbourne, Victoria, Australia in 2014. He completed his B.Sc. and M.Sc. in Mechanical Engineering from Bangladesh University of Engineering and Technology (BUET), Dhaka, Bangladesh on 2004 and 2007, respectively. His major field of study is numerical analysis on problems of thermo-fluid. He is now working as a Professor in the Department of Mechanical Engineering of Bangladesh University of Engineering and Technology (BUET). He already published more than 140 research papers in International Journals and Conference Proceedings and coauthor of two books in engineering field. His fields of interests are turbulent flows, computational fluid mechanics, computational heat transfer and thermal postbuckling analysis. Dr. Saha is the editor of one international journal and reviewers of several international conference proceedings and international journals. He is currently senior member of International Association of Computer Science and Information Technology (IACSIT), Singapore. Moreover, he is a life member of Bangladesh Solar Energy Society. He has received many professional awards like International Postgraduate Research Scholarship by the Australian federal government; Melbourne International Research Scholarship by the University of Melbourne; RHD Studentship by University of Melbourne, and so on.